Organometallics **1997,** *16,* 3993−4000

Insertion Reactions of Tantalum(V) Carborane Alkyl and Aryl Complexes with Nitriles and Isonitriles. Thermal and Photochemical Isomerization of η^2-Iminoacyl Isomers[1]

Eric Boring, Michal Sabat, M. G. Finn,* and Russell N. Grimes*

Department of Chemistry, University of Virginia, Charlottesville, Virginia 22901

Received April 22, 1997[⊗]

Tantalum carborane complexes $(Et_2C_2B_4H_4)CpTaR_2$ (R = Me, Ph) undergo insertion reactions with nitriles and isonitriles under conditions that differ from formally isoelectronic metallocene compounds of group 4 metals. The dimethyltantalum system requires UV−vis irradiation, whereas the diphenyltantalum complex generally reacts at elevated temperatures. Although insertions of isonitriles into metal−alkyl bonds have been reported in a wide variety of cases, there are very few examples of stable isomeric η^2-iminoacyl intermediates that can be isolated and completely converted from one form into the other. Two such cases are reported here, including the X-ray crystallographic analysis of both isomers of $(Et_2C_2B_4H_4)CpTaCH_3(\eta^2\text{-}C,N\text{-}C\{{=}N\text{-}t\text{-}Bu\}CH_3)$ (**5a**,**5b**) and one isomer of $(Et_2C_2B_4H_4)CpTaCH_3(\eta^2\text{-}C,N\text{-}C\{{=}N(2,6\text{-}Me_2C_6H_3)\}C_6H_5)$ (**7a**). Photochemical isomerization of **7a**, followed by exposure to an additional equivalent of isocyanide, resulted in a novel cage-insertion reaction to give $[(Et_2C_2B_4H_3(C_6H_5)(CHN(2,6\text{-}Me_2C_6H_3))]CpTa(\eta^2\text{-}C,N\text{-}C\{{=}N\text{-}(2,6\text{-}Me_2C_6H_3)\}C_6H_5)$ (**8**), the crystal structure of which was also determined. Stereoelectronic and steric factors that may contribute to the thermodynamic stability of N-out isomers of η^2-iminoacyl complexes are suggested, and data indicating the relatively electron-rich nature of the (carborane)(Cp)Ta^VR_2 fragment is identified.

Introduction

The exceedingly rich nature of the chemistry of early transition metal cyclopentadienyl complexes has spawned a growing interest in systems in which Cp is replaced by analogous ligands that exhibit different steric and/or electronic properties.[2−5] We have recently described the synthesis and structural characterization of a variety of halo and alkyl complexes bearing 2,3-$R_2C_2B_4H_4^{2-}$ or 1,2,3-$Cp^*Co(R_2C_2B_4H_4)^{2-}$ ligands, both types of which present a planar C_2B_3 face for η^5-binding to metal ions.[6] In general, the carborane ligands serve to stabilize reactive metal centers, particularly those in high oxidation states, to a far greater degree than $C_5R_5^-$.[7] Among the relevant properties are the difference in overall charge, the greater electropositive nature of boron compared to carbon, and the geometry of the orbitals involved in metal binding. Indeed, it is important to recognize that η^5-C_2B_3 metal species can be regarded as cluster compounds with as much validity as they can be classified as coordination complexes.

In an effort to map the organometallic reactivity of such early metal systems, we have examined and report here the reactions of $(Et_2C_2B_4H_4)CpTaR_2$ compounds (R = Me, Ph)[6,7] with nitriles and isonitriles. We have found that the former undergo photochemical insertion into the metal−carbon bond whereas the latter react cleanly under thermal conditions. Thermal and photochemical isomerizations between product η^2-iminoacyl stereoisomers are observed, as is a novel double insertion process whereby the new organic fragment becomes incorporated in a carborane cage structure. For the first time, both isomers of an η^2-iminoacyl complex have been crystallographically characterized, revealing both steric and stereoelectronic factors that may contribute to their relative stabilities.

Results

The tantalum(V) dimethyl complex **1** was found to be inert when heated (90 °C, 24 h) with an excess of either diphenyl or dimethyl acetylenedicarboxylate.[8] In contrast, insertions of 2-butyne, 3-hexyne, and diphenylacetylene into the $Ta-CH_3$ bond are observed upon photolysis of **1** in the presence of an excess of each alkyne (Scheme 1). We have previously described the conversion of diphenyl complex **2** to a stable benzyne adduct upon heating in the presence of triphenylphosphine.[7] In the absence of phosphine and the presence of alkynes, thermolysis provides five-membered metallacycles derived from the addition of alkyne to a reactive

---

[⊗] Abstract published in *Advance ACS Abstracts,* August 1, 1997.

[1] Organotransition-Metal Metallacarboranes. 50. Part 49: Curtis, M. A.; Finn, M. G.; Grimes, R. N. *J. Organomet. Chem.*, in press.

[2] (a) Rodriguez, G.; Bazan, G. C. *J. Am. Chem. Soc.* **1997**, *119*, 343−352 and references therein. (b) Crowther, D. J.; Baenziger, N. C.; Jordan, R. F. *J. Am. Chem. Soc.* **1991**, *113*, 1455−1457.

[3] Lubben, T. V.; Wolczanski, P. T.; Van Duyne, G. D. *Organometallics* **1984**, *3*, 977−983.

[4] Schafer, V.; Pritzkow, H.; Siebert, W. *Angew. Chem., Int. Ed. Engl.* **1988**, *27*, 299−300.

[5] Kuhn, N.; Horn, E.-M.; Zauder, E.; Blaser, D.; Boese, R. *Angew. Chem., Int. Ed. Engl.* **1988**, *27*, 579−580.

[6] Stockman, K. E.; Houseknecht, K. L.; Boring, E. A.; Sabat, M.; Finn, M. G.; Grimes, R. N. *Organometallics* **1995**, *14*, 3014−3029.

[7] Houseknecht, K. L.; Stockman, K. E.; Sabat, M.; Finn, M. G.; Grimes, R. N. *J. Am. Chem. Soc.* **1995**, *117*, 1163−1164.

[8] We have reported the conversion of diphenyl complex **2** to a stable benzyne adduct when heated in the presence of triphenylphosphine.[7]

S0276-7333(97)00344-0 CCC: $14.00

Scheme 1

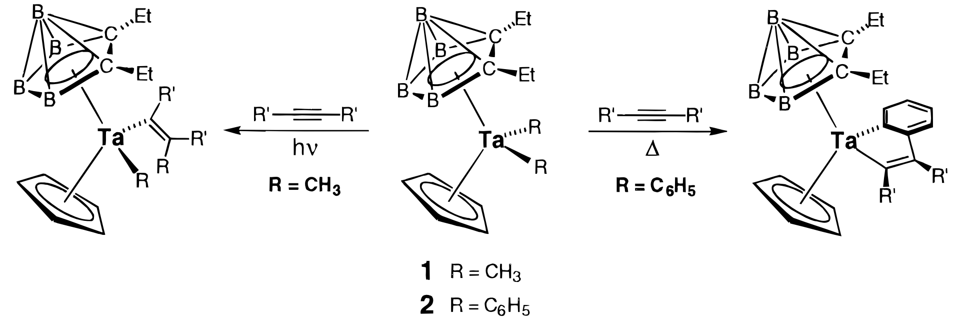

Scheme 2

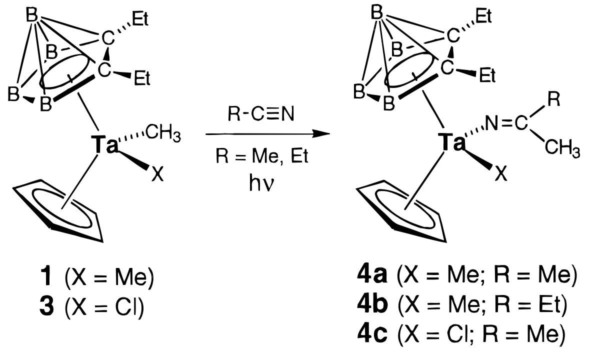

benzyne intermediate, analogous to the chemistry of related zirconocene systems (Scheme 1).[9,10] These transformations of alkynes and subsequent reactions of the resulting metallacarborane complexes will be described separately.

Complex **1** is stable when heated in nitrile solvents. However, when irradiated in acetonitrile or propionitrile solution, **1** provides the azaalkenylidine complexes **4a** and **4b** in high yield (Scheme 2). The chloride complex **3** reacts similarly with acetonitrile to give **4c**. The azaalkenylidene ligands of **4a**−**c** show Ta−N=C ^{13}C NMR resonances (114−129 ppm) considerably upfield from those of analogous cationic zirconocene structures, such as $Cp_2Zr(N{=}C(Me_2)(MeCN)^+$ (180.9 ppm), while the N=C stretching frequencies of **4a** and **4c** (1722, 1690 cm^{-1}, respectively) are at higher energy than that for the zirconocene system (1685 cm^{-1}).[11] The appearance of distinct NMR resonances for the azaalkenylidene methyl groups of **4a** and **4c** demonstrates that rotation about the Ta−N=C bond is slow relative to the NMR time scale, as observed for the zirconocene complex.[11]

In contrast to the low reactivity with alkynes and nitriles, isonitriles insert rapidly at room temperature into the Ta−C bonds of both **1** and **2**. Thus, *tert*-butyl isonitrile reacts within minutes with an equimolar amount of **1** to give a 4:1 ratio of isomeric η^2-iminoacyl complexes **5a** and **5b** (Scheme 3).[12] The major isomer **5a** can be separated from **5b** by multiple recrystallizations. Although stable at room temperature for extended periods, the original product mixture is isomerized completely to **5b** when heated at 60 °C for 24 h.[13] X-ray crystal structures of both isomers (Figures 1 and 2; Table 1) show the expected bent-metallocene structure (the angle between Cp and C_2B_3 planes is 51.8° and 50.3° for **5a** and **5b**, respectively) and opposite orientations of the η^2-*N*-*tert*-butyliminoacyl fragment in the plane bisecting the metallocene unit. Complex **5a** assumes the "proximal" or "N-out" configuration while **5b** can be designated "distal" or "N-in", deriving from the arrangement of the iminoacyl and methyl ligands bound to tantalum in the central plane.[14] An examination of these structures shows that **5a** suffers a destabilizing steric interaction of the *tert*-butyl group with the carborane and Cp fragments, whereas in structure **5b** the interaction of the *tert*-butyl group with its nearest neighbors (Ta−CH_3 and carborane ethyl) is less severe. Complex **5a** displays the shorter Ta−N bond, whereas **5b** has the shorter Ta−C(iminoacyl) interaction. The compounds have essentially the same Ta−CH_3 bond distance.

The reaction of **1** with 1 equiv of 2,6-dimethylphenyl isocyanide gives a single η^2-iminoacyl isomer **6** (Scheme 3). Contrary to the *tert*-butyl case, decomposition results when **6** is either heated (90 °C, 24 h) or irradiated (12 h). In analogy to complex **7** (see below), the configuration is **6** is tentatively assigned as N-in.

Scheme 4 shows a series of transformations initiated by an insertion reaction involving diphenyl complex **2**. Treatment with equimolar 2,6-dimethylphenyl isocyanide rapidly provides **7a**, in which a phenyl group has been added to the terminal isocyanide carbon. In this case, only the N-in isomer is formed, as revealed by the X-ray crystal structure of **7a** (Figure 3; Table 2). With respect to the Ta−C4−N1−C10 plane that bisects the "metallocene" moiety, the 2,6-disubstituted aromatic group (C11−C18) is rotated 58°, the unsubstituted iminoacyl phenyl ring (C19−C24) is rotated 23°, and the Ta−phenyl ligand (C4−C9) is rotated 33°.

Complex **7a** is stable toward heating at 60 °C for 12 h but decomposes at higher temperatures. No reaction with excess 2,6-dimethylphenyl isocyanide, diphenylacetylene, or 2-butyne occurs at 60 or 85 °C prior to decomposition. When irradiated for 4 h, **7a** is cleanly isomerized to the N-out isomer **7b**, as indicated by NMR

---

(9) Broene, R. D.; Buchwald, S. L. *Science* **1993**, *261*, 1696−1701.

(10) Buchwald, S. L.; Nielsen, R. B. *Chem. Rev.* **1988**, *88*, 1047−1058.

(11) Alelyunas, Y. W.; Jordan, R. F.; Echols, S. F.; Borkowsky, S. L.; Bradley, P. K. *Organometallics* **1991**, *10*, 1406−1416 and references therein.

(12) The niobium analogue of dimethyl complex **1** undergoes the same transformation with *tert*-butyl isocyanide, giving a 14:1 ratio of isomers, which is stable toward heating at 90 °C for several hours. The structure of the major isomer has not been determined conclusively, but the NMR trends match those observed for **5a** vs **5b**.

(13) Under analogous conditions, complex **1** reacts with benzyl isocyanide to give a mixture of two products in varying ratios depending on the amount of isocyanide used. The major isomer is the same in all cases, and the minor species is completely converted to the major one upon heating at 65 °C. Mass spectrometry confirms the incorporation of one isocyanide unit in each molecule. Although we have not fully characterized these species, their NMR spectra strongly suggest the formation of η^2-iminoacyl complexes analogous to **5** and **6** and a thermal conversion analogous to the transformation of **5a** to **5b**.

(14) Durfee, L. D.; Rothwell, I. P. *Chem. Rev.* **1988**, *88*, 1059−1079.

Scheme 3

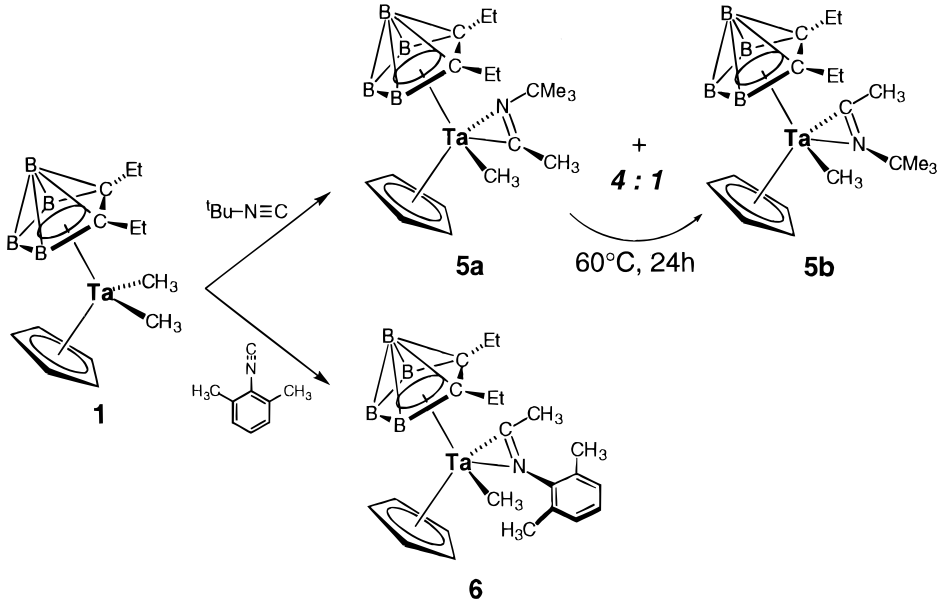

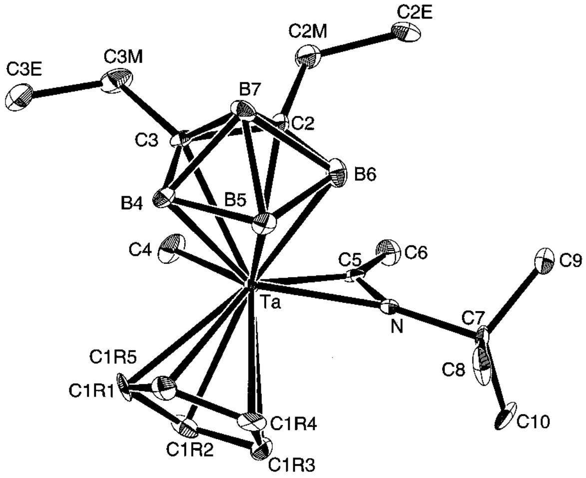

Figure 1. ORTEP drawing of the solid state structure of **5a** showing 30% probability ellipsoids with atom numbering scheme. H atoms are omitted for clarity.

measurements. Although **7b** alone decomposes when heated to 60 °C in benzene solvent, no reaction occurs upon heating with diphenylacetylene or 2-butyne. However, reaction with 1 equiv of 2,6-dimethylphenyl isocyanide or *tert*-butyl isocyanide is fast at room temperature, affording complexes **8** and **9**, respectively. Figure 4 (Table 3) shows the X-ray crystal structure of **8**, revealing that a variety of transformations has occurred. Instead of undergoing a second insertion into the remaining Ta−phenyl bond, the added isocyanide inserts into the Ta−carborane cage so that only B5 and B6 of the carborane have direct contact with tantalum. The terminal isocyanide carbon bridges between carborane C2, B6, and the metal, and the former Ta−phenyl ligand is found attached to the central ring boron (B5). The structure of **9** is assigned to be analogous to that of **8** on the basis of the resemblance between the sets of NMR data for each.[15]

Discussion

The insertion of unsaturated organic compounds into metal−carbon bonds is a well-known process that is an important step in a many stoichiometric and catalytic transformations. Since the C_2B_3 fragment is highly stabilizing toward a variety of metal centers,[6,16−20] we anticipated that discrete insertion steps could be easily studied using (carborane)CpTaR_2 and related systems.

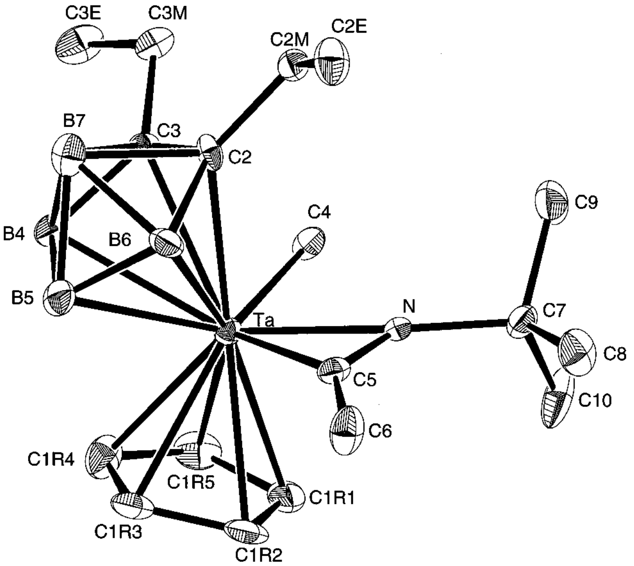

Figure 2. ORTEP drawing of the solid state structure of **5b** showing 30% probability ellipsoids with atom numbering scheme. H atoms are omitted for clarity.

---

[15] In contrast to the reaction of **7b**, complex **6** (Scheme 3) is unchanged upon treatment with 2,6-dimethylphenyl isocyanide at room temperature. However, when **6** is photolyzed in the presence of the isocyanide, four organometallic products are formed. These compounds were separated by preparative thin layer chromatography and shown by mass spectometry to have identical molecular weights corresponding to a 1:1 addition of the reaction components, but detailed structures cannot be proposed with the available data. It is likely that cage insertion chemistry similar to that shown in Scheme 4 also occurs in this case, since one of these isolated products displays a broadened singlet corresponding to a methyl group attached to boron. Similarly, complexes **5a** and **5b** do not react with excess *t*-BuNC at room temperature but do undergo reaction upon photolysis to give several products, which were also shown by mass spectrometry to incorporate one additional equivalent of isocyanide.

(16) Grimes, R. N. *Chem. Rev.* **1992**, *92*, 251−268.

(17) Siebert, W. *Pure Appl. Chem.* **1987**, *59*, 947−954.

(18) Stockman, K. E.; Sabat, M.; Finn, M. G.; Grimes, R. N. *J. Am. Chem. Soc.* **1995**, *117*, 1163−1164.

(19) Merkert, J. M.; Geiger, W. E.; Attwood, M. D.; Grimes, R. N. *Organometallics* **1991**, *10*, 3545.

(20) Stephan, M.; Davis, J. H., Jr.; Meng, X.; Chase, K. P.; Hauss, J.; Zenneck, U.; Pritzkow, H.; Siebert, W.; Grimes, R. N. *J. Am. Chem. Soc.* **1992**, *114*, 5214−5221.

Table 1. Bond Distances (Å) and Bond Angles (deg) for Complexes 5a and 5b

	5a	**5b**
Ta−N	2.155(6)	2.208(8)
Ta−C(2)	2.428(8)	2.43(1)
Ta−C(3)	2.450(7)	2.49(1)
Ta−C(4)	2.258(8)	2.24(1)
Ta−C(5)	2.157(8)	2.12(1)
Ta−C(1R1)	2.451(7)	2.429(9)
Ta−C(1R2)	2.472(7)	2.43(1)
Ta−C(1R3)	2.467(8)	2.41(1)
Ta−C(1R4)	2.413(7)	2.42(1)
Ta−C(1R5)	2.465(8)	2.44(1)
Ta−B(4)	2.467(9)	2.47(1)
Ta−B(5)	2.45(1)	2.42(1)
Ta−B(6)	2.482(9)	2.42(1)
N−C(5)	1.26(1)	1.25(1)
N−C(7)	1.51(1)	1.51(1)
C(5)−C(6)	1.50(1)	1.51(1)
C(7)−C(8)	1.53(1)	1.49(2)
C(7)−C(9)	1.51(1)	1.52(1)
C(7)−C(10)	1.51(1)	1.50(1)
Ta−C(5)−C(6)	153.2(6)	146.8(8)
Ta−N−C(5)	73.1(5)	69.3(6)
Ta−N−C(7)	153.6(6)	156.6(6)
Ta−C(5)−N	73.0(5)	77.3(6)
C(4)−Ta−C(5)	78.5(3)	115.2(4)
N−Ta−C(4)	112.0(3)	81.8(3)
N−Ta−C(5)	33.9(3)	33.4(3)
N−C(5)−C(6)	133.8(7)	135(1)
C(5)−N−C(7)	133.3(8)	132.6(8)
C(3)−C(2)−B(6)	110.0(7)	113.1(9)
C(2)−B(6)−B(5)	105.5(6)	105(1)
B(4)−B(5)−B(6)	105.8(7)	105.4(8)
C(3)−B(4)−B(5)	106.0(7)	106.3(8)
C(2)−C(3)−B(4)	112.6(7)	121(1)

In contrast to the facile reaction of both neutral and cationic group 4 metallocene alkyls with alkynes,[21−30] (carborane)CpTa complexes **1**−**3** are inert toward simple alkynes at elevated temperatures. Instead, insertion chemistry is photochemically driven. Similarly, the expected reaction of nitriles and tantalum methyl complexes **1** and **3** also results from photolysis (Scheme 2), in this case consistent with the chemistry of neutral isoelectronic bis(cyclopentadienyl) complexes of group 4 which do not insert nitriles under thermal conditions. Cationic zirconocene alkyls are considerably more reactive,[11,31−36] as are hydride[37] and allyl[38] complexes of group 4 and carbene complexes of group 6.[39,40]

The rapid insertion of isonitriles into the Ta−C bonds of both **1** and **2** mirrors the chemistry of many metal alkyl complexes[14,41−44] but relatively few of these are Cp-based.[14,45−47] While N-out and N-in isomers have been seen to interconvert rapidly in zirconocene complexes,[11,48] the formation of stable isomers and their interconversion under well-defined thermal or photochemical conditions, as reported here, is rare for metallocene species.[48,49]

The identification of O-out isomers as the kinetic products of carbon monoxide insertion into metal alkyls has previously been made,[50] and the analogous relationship has frequently been assumed and once demonstrated for isocyanides by the spectroscopic observation of the facile conversion of N-out to N-in η^2-iminoacyl species.[48] The thermal isomerization of **5a** (N-out) to **5b** (N-in) suggests that the latter is the more stable isomer and the former is the kinetically-preferred structure for insertion of *tert*-butyl isocyanide.[51] To our knowledge, both N-in and N-out isomers of the same compound have never before been crystallographically characterized. Particularly interesting is the relatively large change in $d_{\mathrm{M-N}} - d_{\mathrm{M-C}}$ that occurs upon isomerization of **5a** to **5b**. If an unsymmetrical η^2-iminoacyl unit is preferred as discussed below, then **5b** may be more stable for stereoelectronic as well as for steric reasons by virtue of a "relaxation" of the anomalously symmetrical iminoacyl binding in **5a**. Further work, including the structural characterization of the products resulting from reaction of other isocyanides with **1**,[13] is necessary to resolve the relative contributions of steric and electronic factors in these insertions.

The insertion of 2,6-dimethylphenyl isocyanide into the Ta−Ph bond of **2** gives the N-in isomer **7a** exclusively, which can be driven to the N-out structure **7b** by visible light irradiation but not by heating. It is thus not certain if **7a** is preferred for "kinetic" or "thermo-

---

(21) Doxsee, K. M.; Juliette, J. J. J.; Mouser, J. K. M.; Zientara, K. *Organometallics* **1993**, *12*, 4682−4686.

(22) Doxsee, K. M.; Juliette, J. J. J.; Zientara, K.; Nieckarz, G. *J. Am. Chem. Soc.* **1994**, *116*, 2147−2148.

(23) Horton, A. D.; Orpen, A. G. *Organometallics* **1991**, *10*, 3910−3918.

(24) Leong, W. W.; Larock, R. C. In *Comprehensive Organometallic Chemistry II*; Hegedus, L. S., Ed.; Pergamon: Oxford, U.K. 1995; Vol. 12, Chapter 3.3, pp 131−160.

(25) Bochmann, M. In *Comprehensive Organometallic Chemistry II*; Lappert, M. F., Ed.; Pergamon: Oxford, U.K. 1995; Vol. 4, Chapter 5, pp 273−431.

(26) Soderberg, B. C. In *Comprehensive Organometallic Chemistry II*; Hegedus, L. S., Ed.; Pergamon: Oxford, U.K. 1995; Vol. 12, Chapter 3.5, pp 241−297.

(27) Grigg, R.; Sridharan, V. In *Comprehensive Organometallic Chemistry II*; Hegedus, L. S., Ed.; Pergamon: Oxford, U.K. 1995; Vol. 12, Chapter 3.6, pp 299−321.

(28) Jubb, J.; Song, J.; Richeson, D.; Gambarotta, S. In *Comprehensive Organometallic Chemistry II*; Lappert, M. F., Ed.; Pergamon: Oxford, U.K. 1995; Vol. 4, Chapter 11, pp 543−588.

(29) Thebtavanonth, C.; Thebtavanonth, Y. In *Cyclization Reactions*; CRC Press: Ann Arbor, MI, 1994; pp 255−330.

(30) Negishi, E.-I.; Takahashi, T. *Acc. Chem. Res.* **1994**, *27*, 124−130.

(31) Michelin, R. A.; Mozzon, M.; Bertani, R. *Coord. Chem. Rev.* **1996**, *147*, 299−338.

(32) Alelyunas, Y. W.; Guo, Z. Y.; Lapointe, R. E.; Jordan, R. F. *Organometallics* **1993**, *12*, 544−553.

(33) Bochmann, M.; Wilson, L. M.; Hursthouse, M. B.; Motevalli, M. *Organometallics* **1988**, *7*, 1148−1154.

(34) Doxsee, K. M.; Farahi, J. B. *J. Chem. Soc., Chem. Commun.* **1990**, 1452−1454.

(35) Hylakryspin, I.; Niu, S. Q.; Gleiter, R. *Organometallics* **1995**, *14*, 964−974.

(36) For nitrile coupling reactions, see also: Doxsee, K. M.; Juliette, J. J. J.; Mouser, J. K. M.; Zientara, K. *Organometallics* **1993**, *12*, 4682−4686. Alvarado, Y.; Daff, P. J.; Perez, P. J.; Poveda, M. L.; Sanchezdelgado, R.; Carmona, E. *Organometallics* **1996**, *15*, 2192−2194. Temme, R.; Erker, G. *J. Organomet. Chem.* **1995**, *488*, 177−182.

(37) Erker, G.; Fromberg, W.; Atwood, J. L.; Hunter, W. E. *Angew. Chem., Int. Ed. Engl.* **1984**, *23*, 68−69.

(38) Klei, E.; Teuben, J. H.; de Liefde Meijer, H. J. *J. Chem. Soc., Chem. Commun.* **1981**, 342−344.

(39) Fischer, H.; Markl, R.; Zeuner, S. *J. Organomet. Chem.* **1985**, *286*, 17−26.

(40) Yang, D. C.; Dragisich, V.; Wulff, W. D.; Huffman, J. C. *J. Am. Chem. Soc.* **1988**, *110*, 307−309.

(41) Knight, D. A.; Dewey, M. A.; Stark, G. A.; Bennett, B. K.; Arif, A. M.; Gladysz, J. A. *Organometallics* **1993**, *12*, 4523−4534.

(42) Jacoby, D.; Isoz, S.; Floriani, C.; Schenk, K.; Chiesi-Villa, A.; Rizzoli, C. *Organometallics* **1995**, *14*, 4816−4824.

(43) Ito, Y. *Pure Appl. Chem.* **1990**, *62*, 583−588.

(44) Carofiglio, T.; Floriani, C.; Chiesi-Villa, A.; Guastini, C. *Inorg. Chem.* **1989**, *28*, 4417−4419.

(45) Guram, A. S.; Jordan, R. F. *J. Org. Chem.* **1993**, *58*, 5595−5597.

(46) Honda, T.; Satoh, S.; Mori, M. *Organometallics* **1995**, *14*, 1548−1550.

(47) Curtis, M. D.; Real, J.; Hirpo, W.; Butler, W. M. *Organometallics* **1990**, *9*, 66−74.

(48) Lemke, F. R.; Szalda, D. J.; Bullock, R. M. *Organometallics* **1992**, *11*, 876−884. See references herein for several examples of the fluxional interconversion of η^2-iminoacyl isomers.

(49) An example of the formation and separation, but not interconversion, of the two isomers of a niobocene halide η^2-iminoacyl system is provided. See: Antiñolo, A.; Fajardo, M.; Gil-Sanz, R.; López-Mardomingo, C.; Martín-Villa, P.; Otero, A.; Kubicki, M. M.; Mugnier, Y.; El Krami, S.; Mourad, Y. *Organometallics* **1993**, *12*, 381−388.

(50) Erker, G. *Acc. Chem. Res.* **1984**, *17*, 103−109.

(51) However, **5a** cannot definitively be assigned as the "kinetic" product since the same 4:1 ratio of isomers is obtained when the reaction is conducted at −78 °C.

Scheme 4

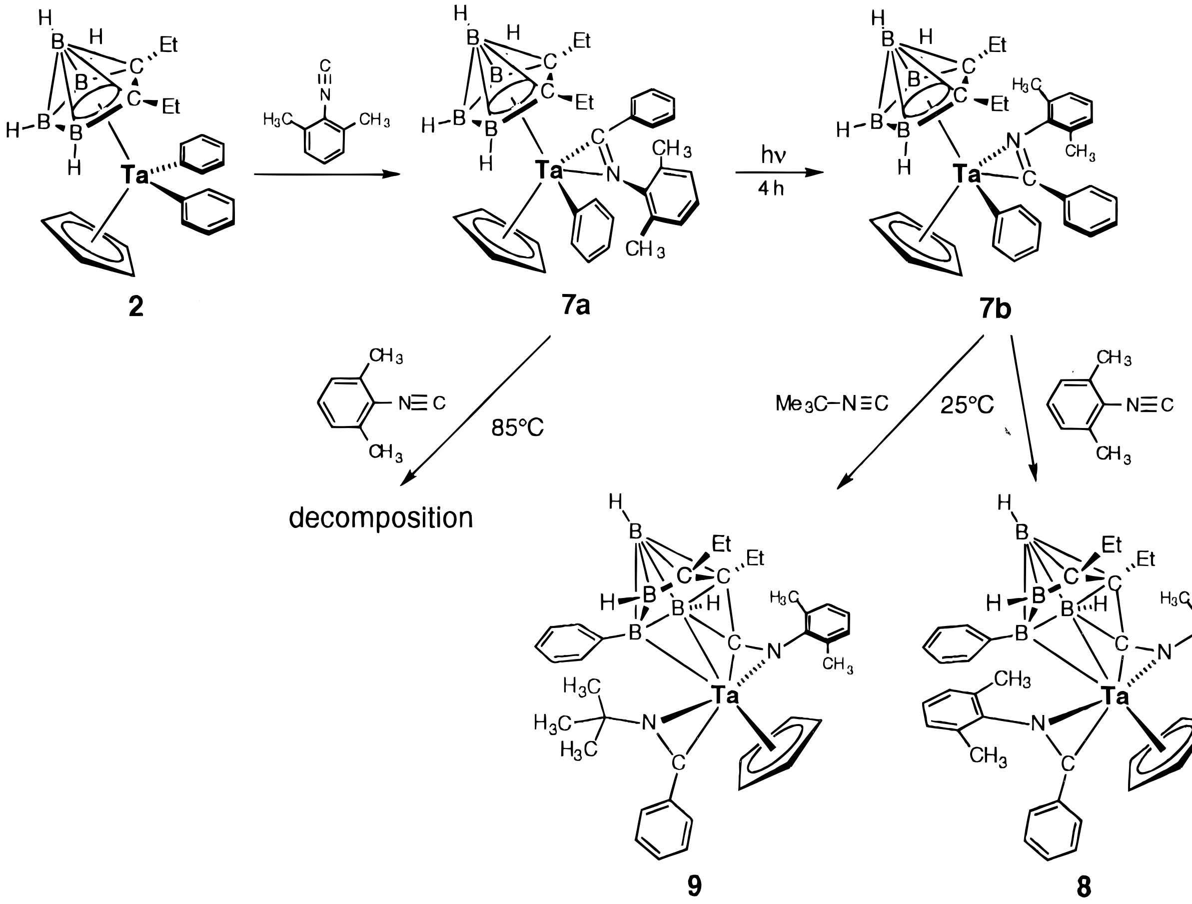

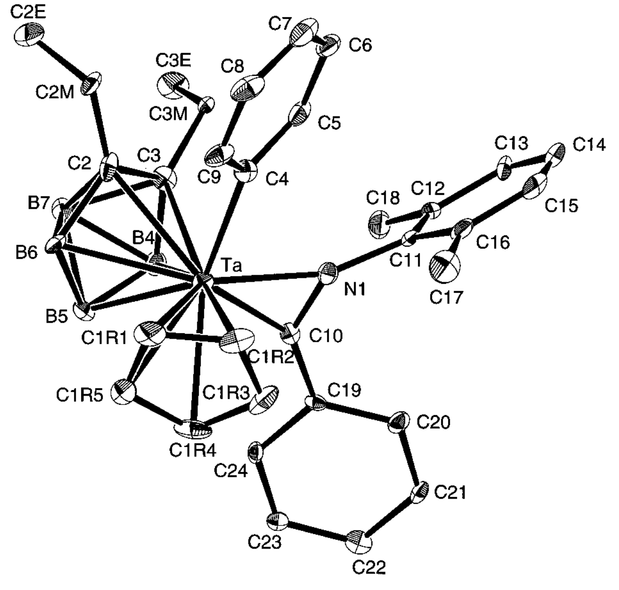

Figure 3. ORTEP drawing of the solid state structure of **7a** showing 30% probability ellipsoids with atom numbering scheme. H atoms are omitted for clarity.

dynamic" reasons or both. In analogy to other systems and given the greater reactivity of **7b** toward additional isocyanide, we assume that **7a** is the thermodynamically preferred isomer. The present report is thus the first example of the selective generation of an N-out η^2-iminoacyl isomer by photoisomerization.

The difference in reactivity of isomers **7a** and **7b** toward isocyanide is profound: **7a** resists reaction with 2,6-dimethylphenyl isocyanide at 85 °C whereas **7b** reacts immediately at room temperature. Multiple isocyanide insertions are known for a variety of metal alkyl complexes but not for bis(Cp)-bound and related metal centers, presumably because space around the metal center is not available to accomodate two η^2-iminoacyl ligands. The (carborane)(Cp)Ta system is no exception, but the carborane fragment provides an alternative cage insertion reaction pathway for added isocyanide.[52] We speculate that isocyanide can interact directly with the Ta−carborane unit with subsequent phenyl transfer from tantalum to boron. If such a pathway requires attack of isocyanide next to the Ta−Ph bond, then the bulky 2,6-dimethylphenyl group next to the phenyl ligand would block the transformation of **7a**, whereas such an unfavorable interaction is not present in the reactive isomer **7b**. Of course, **7b** is also

Table 2. Bond Distances (Å) and Bond Angles (deg) for Complex 7a

Ta−N(1)	2.218(6)	Ta−C(1R4)	2.453(7)
Ta−C(2)	2.453(8)	Ta−C(1R5)	2.458(7)
Ta−C(3)	2.434(7)	Ta−B(4)	2.452(8)
Ta−C(4)	2.287(7)	Ta−B(5)	2.432(9)
Ta−C(10)	2.145(7)	Ta−B(6)	2.476(8)
Ta−C(1R1)	2.402(7)	N(1)−C(10)	1.259(9)
Ta−C(1R2)	2.407(7)	N(1)−C(11)	1.474(9)
Ta−C(1R3)	2.470(8)	C(10)−C(19)	1.46(1)
Ta−C(10)−C(19)	149.3(5)	N(1)−C(10)−C(19)	133.0(6)
Ta−N(1)−C(10)	70.1(4)	C(10)−N(1)−C(11)	133.6(6)
Ta−N(1)−C(11)	156.3(5)	C(3)−C(2)−B(6)	111.6(6)
Ta−C(10)−N(1)	76.4(4)	C(2)−B(6)−B(5)	104.9(6)
C(4)−Ta−C(10)	116.9(3)	B(4)−B(5)−B(6)	106.1(6)
N(1)−Ta−C(4)	83.4(2)	C(3)−B(4)−B(5)	104.1(6)
N(1)−Ta−C(10)	33.5(2)	C(2)−C(3)−B(4)	113.3(6)

---

[52] Also not observed is the coupling of added isocyanide to the η^2-iminoacyl ligand to give metallacycle intermediates. See: Filippou, A. C.; Volkl, C.; Kiprof, P. *J. Organomet. Chem.* **1991**, *415*, 375−394.

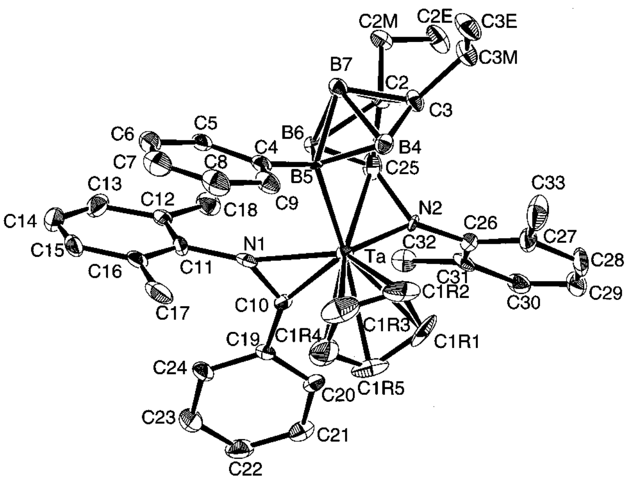

Figure 4. ORTEP drawing of the solid state structure of **8** showing 30% probability ellipsoids with atom numbering scheme. H atoms are omitted for clarity.

Table 3. Bond Distances (Å) and Bond Angles (deg) for Complex 8

Ta−N(1)	2.202(6)	C(2)−C(25)	1.66(1)
Ta−N(2)	1.949(5)	C(25)−B(6)	1.73(1)
Ta−C(10)	2.133(7)	C(2)−B(6)	1.75(1)
Ta−C(25)	2.411(9)	C(2)−B(7)	1.70(1)
Ta−B(5)	2.296(7)	C(3)−B(4)	1.52(1)
Ta−B(6)	2.410(8)	C(3)−B(7)	1.65(1)
Ta−C(1R1)	2.436(8)	C(4)−B(5)	1.50(1)
Ta−C(1R2)	2.368(9)	C(1R1)−C(1R2)	1.50(2)
Ta−C(1R3)	2.40(1)	C(1R1)−C(1R5)	1.41(2)
Ta−C(1R4)	2.47(1)	C(1R2)−C(1R3)	1.37(2)
Ta−C(1R5)	2.511(9)	C(1R3)−C(1R4)	1.26(2)
N(1)−C(10)	1.314(9)	C(1R4)−C(1R5)	1.32(2)
N(1)−C(11)	1.44(1)	B(4)−B(5)	1.60(1)
N(2)−C(25)	1.51(1)	B(4)−B(7)	1.77(1)
N(2)−C(26)	1.429(9)	B(5)−B(6)	1.63(1)
C(10)−C(19)	1.48(1)	B(5)−B(7)	1.72(1)
C(2)−C(3)	1.49(1)	B(6)−B(7)	1.80(1)
Ta−C(10)−C(19)	155.4(5)	Ta−B(5)−B(7)	125.5(5)
Ta−−N(1)−C(10)	69.5(4)	C(4)−B(5)−B(4)	118.6(6)
Ta−N(1)−C(11)	160.3(5)	C(4)−B(5)−B(6)	124.9(6)
Ta−N(2)−C(25)	87.5(4)	C(4)−B(5)−B(7)	109.9(6)
Ta−N(2)−C(26)	144.0(5)	B(4)−B(5)−B(6)	107.8(6)
N(1)−C(10)−C(19)	129.0(7)	B(4)−B(5)−B(7)	64.5(5)
Ta−C(10)−N(1)	75.3(4)	B(6)−B(5)−B(7)	64.8(5)
Ta−C(25)−N(2)	53.8(3)	C(2)−B(6)−B(5)	102.1(6)
Ta−C(25)−C(2)	110.7(5)	C(3)−C(2)−B(6)	107.0(6)
Ta−C(25)−B(6)	69.0(4)	C(2)−C(3)−B(4)	113.1(6)
N(2)−C(25)−C(2)	120.1(6)	C(3)−B(4)−B(5)	108.5(6)
N(2)−C(25)−B(6)	119.8(6)	Ta−B(6)−C(2)	107.5(4)
C(25)−N(2)−C(26)	126.1(6)	Ta−B(6)−C(25)	69.1(4)
Ta−B(5)−C(4)	122.6(5)	Ta−B(6)−B(5)	66.0(4)
Ta−B(5)−B(4)	99.1(4)	C(2)−B(6)−C(25)	57.0(4)
Ta−B(5)−B(6)	73.5(4)	C(25)−B(6)−B(5)	119.7(6)

the higher-energy structure, being generated only by photolysis of **7a**, and may suffer other types of steric and/or stereoelectronic destabilization.

A correlation between the electronic properties of the metal center and the symmetry of the metal interaction with the η^2-iminoacyl fragment has been identified, in analogy to similar findings for η^2-acyl complexes.[14] The quantity $d_{\mathrm{M-N}} - d_{\mathrm{M-C}}$ ranges from approximately 0.10 to −0.22 Å, with positive values characteristic of electron-rich systems and negative values exhibited by electron-poor complexes.[53] Except for **5a**, the structures described here show relatively large values for metal complexes of the formal d^0 oxidation state (**5a**, −0.002 ± 0.014 Å; **5b**, 0.09 ± 0.02 Å; **7a**, 0.073 ± 0.013 Å; **8**, 0.069 ± 0.013 Å). Similar results are reported for a porphyrinogen complex of Nb(IV) (0.074 Å),[53a] an arylthiolate complex of $Cp_2Zr(IV)$ (0.065 Å),[53c] and an aryloxide complex of $Cp_2Zr(IV)$ (0.036 Å),[14] all of which contain strongly electron-donating ligands. By this measure, the metallacarborane unit is revealed to be highly electron-rich for its formal oxidation state, which is consistent with the nonexistent or sluggish insertion chemistry discussed above relative to the fast insertion reactions of cationic metallocene systems.[45] As shown here, the carborane fragment frequently imposes kinetic, but not thermodynamic, barriers to insertion and isomerization processes, an unusual property that may be generally useful for the study and regulation of other reaction pathways.

Experimental Section

^{1}H (300 MHz), ^{11}B (115.8 MHz), and ^{13}C (75.5 and 125.3 MHz) NMR spectra were acquired on Nicolet NT-360 and GE QE-300 instruments. Unless otherwise noted, the ^{1}H NMR spectra of all new carborane complexes display ethyl CH_2 signals as doublets of quartets with coupling constants of 15 and 7.5 Hz and ethyl CH_3 as triplets with $J = 7.5$ Hz. UV−vis spectra were recorded on a Hewlett-Packard 8452A diode array spectrophotometer. Unit resolution mass spectra were obtained on a Finnegan MAT 4600 spectrometer using perfluorotributylamine (FC43) as the calibration standard. In all cases, strong parent ion envelopes were observed and the observed and calculated spectral patterns were in close agreement. Elemental analyses were obtained in this department on a Perkin-Elmer 2400 CHN Analyzer using 2,4-dinitrophenylhydrazone as the calibration standard. Infrared spectra were recorded as thin films on a Mattson Cygnus FTIR spectrometer. Photolyses were performed in Pyrex flasks using a water-cooled Hanovia mercury arc lamp. All solvents were distilled under a dry nitrogen atmosphere from Na/benzophenone. $(Et_2C_2B_4H_4)(C_5H_5)Ta(CH_3)_2$ (**1**), $(Et_2C_2B_4H_4)(C_5H_5)Ta(C_6H_5)_2$ (**2**), and $(Et_2C_2B_4H_4)(C_5H_5)Ta(Cl)(CH_3)$ (**3**) were prepared as previously described.[6] All other reagents were purchased and used as received. Unless otherwise indicated, reactions and purifications were performed in air.

$(Et_2C_2B_4H_4)CpTaCH_3[N{=}C(CH_3)_2]$ (4a). Complex **1** (100 mg, 0.247 mmol) was dissolved in 5 mL of dry deoxygenated acetonitrile in a Pyrex flask and irradiated under nitrogen for 70 min, resulting in a dark yellow solution. The residue obtained after removal of the solvent by rotary evaporation was dissolved in dichloromethane and filtered through Celite. Rotary evaporation provided **4a** as a light brown oil (67 mg, 61%). ^{1}H NMR ($CDCl_3$, δ): 5.72 (s, 5H), 2.60 (m, 2H), 2.34 (m, 2H), 1.81 (s, 3H), 1.76 (s, 3H), 1.19 (t, 3H), 1.15 (t, 3H), 0.05 (s, 3H). ^{13}C NMR ($CDCl_3$, δ): 129.1, 107.1, 29.2, 28.3, 24.6, 23.6, 23.2, 14.9, 14.7. ^{11}B NMR ($CDCl_3$, δ): 20.3 (d, $J =$ 163 Hz, 1B), 16.5 (d, $J = 140$ Hz, 1B), 16.1 (d, $J = 135$ Hz, 1B), −3.4 (d, $J = 165$ Hz). IR (CH_2Cl_2, cm^{-1}): 3118 (w), 2540 (s), 1722 (m), 1375 (m), 1281 (s), 1124 (w), 1080 (w), 778 (m), 708 (w). UV−vis (CH_2Cl_2, nm): 310 (63%), 254 (75%), 216 (100%). MS (CI using CH_4): *m/z* 467 (base peak; molecular ion envelope). Anal. Calcd for $C_{15}H_{28}NB_4Ta$: C, 40.34; H, 6.32; N, 3.14. Found: C, 40.45; H, 6.21; N, 3.23.

---

(53) For recent examples, see: (a) porphyrinogen complexes of Nb(V); $d_{\mathrm{M-N}} - d_{\mathrm{M-C}} = 0.074$ Å. Isoz, S.; Floriani, C.; Schenk, K.; Chiesi-Villa, A.; Rizzoli, C. *Organometallics* **1996**, *15*, 337−344. (b) porphyrinogen complex of Zr(IV); $d_{\mathrm{M-N}} - d_{\mathrm{M-C}} = 0.010$ Å. Jacoby, D.; Isoz, S.; Floriani, C.; Schenk, K.; Chiesi-Villa, A.; Rizzoli, C. *Organometallics* **1995**, *14*, 4816−4824. (c) Bis(Cp) arylthiolate Zr(IV); $d_{\mathrm{M-N}} - d_{\mathrm{M-C}} =$ 0.065 Å. Fandos, R.; Lanfranchi, M.; Otero, A.; Pellinghelli, M. A.; Ruiz, M. J.; Terreros, P. *Organometallics* **1996**, *15*, 4725−4730. (d) Cyclic metallocene−alkyl complexes of Zr(IV) and Hf(IV); $d_{\mathrm{M-N}} - d_{\mathrm{M-C}} =$ 0.015, 0.023 Å. Berg, F. J.; Petersen, J. L. *Organometallics* **1993**, *12*, 3890−3895. (e) Bis(pyrazolyl)borate carbonyl phosphine complexes of Mo(II); $d_{\mathrm{M-N}} - d_{\mathrm{M-C}} = 0.005$ Å. Pizzano, A.; Sánchez, L.; Altmann, M.; Monge, A.; Ruiz, C.; Carmona, E. *J. Am. Chem. Soc.* **1995**, *117*, 1759−1765. (f) Arylmolybdenum(V) carbonyl dimers; $d_{\mathrm{M-N}} - d_{\mathrm{M-C}} =$ −0.038, −0.001 Å. Laï, R.; Desbois, O.; Zamkotsian, F.; Faure, R.; Feneau-Dupont, J.; Declercq, J.-P. *Organometallics* **1995**, *14*, 2145−2147.

$(\mathrm{Et_2C_2B_4H_4})\mathrm{CpTaCH_3[N{=}C(C_2H_5)(CH_3)]}$ (4b). Prepared from **1** and propionitrile using the same procedure as above, **4b** was isolated as a brown oil in 64% yield (89 mg). NMR of this product indicates that **4b** comprises approximately 85% of the sample; further purification has been unsuccessful. ^{1}H NMR ($\mathrm{CDCl_3}$, δ): 5.70 (s, 5H), 2.58 (m, 2H), 2.42 (m, 2H), 2.24 (q, $J = 6.6$ Hz, 2H), 1.96 (s, 3H), 1.19 (t, 3H), 1.16 (t, 3H), 0.85 (t, $J = 7.8$ Hz, 3H), 0.02 (s, 3H). ^{13}C NMR ($\mathrm{CDCl_3}$, δ): 114.9, 105.6, 34.7, 30.3, 28.0, 23.5, 23.1, 20.5, 15.8, 15.5. ^{11}B NMR ($\mathrm{CDCl_3}$, δ): 17.9 (d, $J = 124$ Hz, 1B), 15.8 (d, $J = 134$ Hz, 1B), 14.2 (d, $J = 168$ Hz, 1B), -3.2 (d, $J = 157$ Hz, 1B). MS (CI using $\mathrm{CH_4}$): *m*/*z* 460 (base peak; molecular ion envelope).

$(\mathrm{Et_2C_2B_4H_4})\mathrm{CpTaCl[N{=}C(CH_3)_2]}$ (4c). Prepared from **3** (100 mg, 0.247 mmol) and acetonitrile using the same procedure as above, **4c** was isolated as a yellow brown oil in 71% yield (78 mg). ^{1}H NMR ($\mathrm{CDCl_3}$, δ): 5.97 (s, 5H), 2.88 (m, 1H), 2.68 (m, 1H), 2.55 (m, 1H), 2.36 (m, 1H), 1.99 (s, 3H), 1.95 (s, 3H), 1.16 (t, 6H). ^{13}C NMR ($\mathrm{CDCl_3}$, δ): 130.7, 107.7, 28.5, 25.0, 23.3, 23.1, 14.7, 14.4. ^{11}B NMR ($\mathrm{CDCl_3}$, δ): 19.2 (d, $J = 167$ Hz, 1B), 17.4 (d, $J = 140$ Hz, 1B), 14.9 (d, $J = 148$ Hz, 1B), -2.0 (d, $J = 156$ Hz, 1B). IR ($\mathrm{CH_2Cl_2}$, cm^{-1}): 3105 (w), 2552 (s), 1690 (s), 1436 (m), 1350 (m), 1706 (w), 1073 (w), 834 (s), 752 (w). UV−vis ($\mathrm{CH_2Cl_2}$, nm): 334 (34%), 264 (65%), 232 (100%). MS (CI using $\mathrm{CH_4}$): *m*/*z* 467 (base peak; molecular ion envelope). Anal. Calcd for $\mathrm{C_{14}H_{25}NB_4Ta}$: C, 36.07; H, 5.40; N, 3.00. Found: C, 36.22; H, 5.46; N, 3.08.

$(\mathrm{Et_2C_2B_4})\mathrm{CpTaCH_3}(\eta^2\text{-}C,N\text{-}\mathrm{C}\{{=}\mathrm{N}\text{-}t\text{-}\mathrm{Bu}\}\mathrm{CH_3})$ (5a and 5b). Complex **1** (100 mg, 0.25 mmol) in 3 mL of benzene was treated with a benzene solution of *tert*-butyl isocyanide (22 mg, 0.28 mmol) at room temperature, causing an immediate color change to light yellow. The solution was filtered through Celite and concentrated by rotary evaporation. Recrystallation of the residue from benzene gave **5a** (111 mg, 92%) as a colorless crystalline solid. The ^{1}H NMR spectrum revealed the presence of two products in a 4:1 ratio. Crystals suitable for X-ray analysis were obtained by washing with cold hexane and recrystallizing twice from ether/hexane (83 mg, 69% yield). The mixture was completely converted to the minor isomer **5b** with >90% mass recovery by heating at 60 °C in benzene for 24 h.

For **5a**. ^{1}H NMR ($\mathrm{CDCl_3}$, δ): 5.41 (s, 5H, *Cp*), 2.61 (s, 3H, N=C*Me*), 2.36 (m, 1H), 2.12 (m, 2H), 1.86 (m, 1H), 1.50 (s, 9H, *t*-Bu), 1.08 (t, 3H), 0.89 (t, 3H), 0.11 (s, 3H, Ta-*Me*). ^{13}C NMR ($\mathrm{CDCl_3}$, δ): 221.1, 128.7, 104.6, 61.0, 29.4, 22.7, 22.5, 15.9, 15.5, 14.4. ^{11}B NMR ($\mathrm{CDCl_3}$, δ): 16.2 (d, $J = 132$ Hz, 1B), 12.8 (m, 2B), 4.3 (d, $J = 160$ Hz, 1B). IR ($\mathrm{CH_2Cl_2}$, cm^{-1}): 2534 (s), 2357 (s), 2332 (m), 1684 (m), 1445 (w), 1366 (w), 1193 (m), 1011 (w), 828 (s), 677 (w). UV−vis ($\mathrm{CH_2Cl_2}$, nm): 230 (100%), 278 (29%). MS (CI using $\mathrm{CH_4}$): *m*/*z* 488 (base peak envelope). Anal. Calcd for $\mathrm{C_{18}H_{34}B_4NTa}$ (4:1 mixture of **5a** and **5b**): C, 44.24; H, 7.01; N, 2.87. Found: C, 44.08; H, 7.12; N, 2.73. For pure **5b**. ^{1}H NMR ($\mathrm{CDCl_3}$, δ): 5.31 (s, 5H, *Cp*), 2.98 (s, 3H, N=C*Me*), 2.48 (m, 1H), 2.10 (m, 2H), 1.92 (m, 1H), 1.32 (s, 9H, *t*-Bu), 1.15 (t, 3H), 0.93 (t, 3H), 0.16 (s, 3H, Ta-*Me*). ^{13}C NMR ($\mathrm{CDCl_3}$, δ): 225.1, 131.3, 103.2, 63.2, 30.6, 24.6, 23.1, 15.8, 15.3, 13.9. ^{11}B NMR ($\mathrm{CDCl_3}$, δ): 17.7 (d, $J = 127$ Hz, 1B), 14.3 (d, $J = 168$ Hz, 1B), 12.5 (d, $J = 150$ Hz, 1B), -3.6 (d, $J = 160$ Hz, 1B). IR ($\mathrm{CH_2Cl_2}$, cm^{-1}): 2515 (s), 1678 (m), 1447 (m), 1363 (m), 1193 (m), 1105 (m), 1010 (w), 828 (w), 765 (m), 551 (w). UV−vis ($\mathrm{CH_2Cl_2}$, nm): 240 (72%), 272 (100%). MS (CI using $\mathrm{CH_4}$): *m*/*z* 488 (base peak envelope). Anal. Calcd for $\mathrm{C_{18}H_{34}B_4NTa}$: C, 44.24; H, 7.01; N, 2.87. Found: C, 44.17; H, 7.08; N, 2.93.

$(\mathrm{Et_2C_2B_4})\mathrm{CpTaCH_3}(\eta^2\text{-}C,N\text{-}\mathrm{C}\{{=}\mathrm{N(2,6\text{-}Me_2C_6H_3)}\}\mathrm{CH_3})$ (6). Complex **1** (100 mg, 0.25 mmol) in 3 mL of benzene was treated with a benzene solution of 2,6-dimethylphenyl isocyanide (36 mg, 0.28 mmol) at room temperature, causing an immediate color change to dark yellow. The solution was filtered through Celite and concentrated by rotary evaporation. Recrystallation of the residue from benzene gave **6** (116 mg, 88%) as a colorless crystalline solid. Only one isomer is formed, as judged by the NMR spectra, and heating the compound at 60 °C resulted in decomposition. ^{1}H NMR ($\mathrm{CDCl_3}$, δ): 7.06 (d, $J = 3.6$ Hz, 1H), 7.00 (t, $J = 5.4$ Hz, 1H), 6.98 (d, $J = 6.0$ Hz, 1H), 5.50 (s, 5H), 2.79 (s, 3H), 2.24 (s, 3H), 2.54 (m, 2H), 2.34 (m, 2H), 2.00 (s, 3H), 1.16 (t, 3H), 0.98 (t, 3H), 0.24 (s, 3H). ^{13}C NMR ($\mathrm{CDCl_3}$, δ): 236.1, 139.2, 131.9, 130.9, 129.9, 129.4, 126.5, 104.6 (s, Cp), 24.8 (Ta−$\mathrm{CH_3}$), 24.1, 21.7, 20.3, 19.9, 16.7, 16.3, 15.8. ^{11}B NMR ($\mathrm{CDCl_3}$, δ): 16.3 (m, 2B), 13.8 (d, $J = 147$ Hz, 1B), -3.6 (d, $J = 130$ Hz, 1B). IR ($\mathrm{CH_2Cl_2}$, cm^{-1}): 2521 (s), 1646 (m), 1464 (w), 1369 (w), 1174 (m), 1136 (w), 765 (m). UV−vis ($\mathrm{CH_2Cl_2}$, nm): 236. MS (CI using $\mathrm{CH_4}$): *m*/*z* 537 (base peak envelope). Anal. Calcd for $\mathrm{C_{22}H_{34}NB_4Ta}$: C, 49.23; H, 6.39; N, 2.69. Found: C, 48.57; H, 6.44; N, 2.69.

$(\mathrm{Et_2C_2B_4})\mathrm{CpTa(C_6H_5)}(\eta^2\text{-}C,N\text{-}\mathrm{C}\{{=}\mathrm{N(2,6\text{-}Me_2C_6H_3)}\}\mathrm{C_6H_5})$ (7a). Complex **2** (100 mg, 0.19 mmol) and 2,6-dimethylphenyl isocyanide (27 mg, 0.21 mmol) were combined, and the crude product was isolated as above. Recrystallization from ether/hexane gave **7a** (116 mg, 93%) as red-orange crystals. Only one isomer is formed, as judged by the NMR spectra, and the compound was unchanged upon heating at 60 °C for 12 h. ^{1}H NMR ($\mathrm{CDCl_3}$, δ): 7.87 ($J = 6.3$ Hz, 1H), 7.58 (d, $J = 5.4$ Hz, 2H), 7.49 (t, $J = 7.5$ Hz, 2H), 7.47 (t, $J = 7.5$ Hz, 2H), 7.15 (t, $J = 6.9$ Hz, 1H), 7.13 (t, $J = 5.4$ Hz, 1H), 7.11 (t, $J = 5.4$ Hz, 1H), 7.00 (d, $J = 6.0$ Hz, 2H), 6.98 (d, $J = 6.0$ Hz, 2H), 5.61 (s, 5H), 2.02 (s, 3H), 1.71 (s, 3H), 2.41 (m, 2H), 2.28 (m, 2H), 0.87 (t, 3H), 0.84 (t, 3H). ^{13}C NMR ($\mathrm{CDCl_3}$, δ): 228.6, 174.6, 141.6, 137.9, 135.2, 132.4, 130.4, 129.8, 129.4, 129.0, 128.9, 128.7, 128.1, 127.2, 126.8, 125.2, 123.7, 105.4, 24.1, 21.5, 19.7, 19.4, 15.7, 15.0. ^{11}B NMR ($\mathrm{CDCl_3}$, δ): 19.1 (d, $J = 130$ Hz, 1B), 14.7 (d, $J = 143$ Hz, 1B), 13.1 (d, $J = 147$ Hz, 1B), -0.6 (d, $J = 161$ Hz, 1B). IR ($\mathrm{CH_2Cl_2}$, cm^{-1}): 3055 (w), 2962 (m), 2924 (w), 2867 (w), 2527 (s, B(H)), 2118 (w), 1640 (s), 1450 (m), 1369 (w), 1180 (m), 771(s), 734 (s). UV−vis ($\mathrm{CH_2Cl_2}$, nm): 240 (100%), 334 (8.5%). MS (CI using $\mathrm{CH_4}$): *m*/*z* 659 (base peak envelope). Anal. Calcd for $\mathrm{C_{32}H_{38}NB_4Ta}$: C, 58.16; H, 5.80; N, 2.12. Found: C, 57.72; H, 5.72; N, 2.17.

$(\mathrm{Et_2C_2B_4})\mathrm{CpTa(C_6H_5)}(\eta^2\text{-}C,N\text{-}\mathrm{C}\{{=}\mathrm{N(2,6\text{-}Me_2C_6H_3)}\}\mathrm{C_6H_5})$ (7b). A solution of complex **7a** (116 mg) in 3 mL of benzene was photolyzed under nitrogen for 4 h at room temperature, causing a color change from dark yellow orange to dark red. The residue obtained after the removal of the solvent under vacuum was dissolved in hexane and filtered through Celite, giving a dark red solid after evaporation (101 mg, 81%). ^{1}H NMR ($\mathrm{CDCl_3}$, δ): 8.08 (d, $J = 1.8$ Hz, 2H), 8.06 (d, $J =$ 3Hz, 2H), 7.20 (m, 1H), 7.18 (m, 1H), 7.14 (m, 1H), 7.12 (m, 2H), 7.08 (d, $J = 20.4$ Hz, 1H), 7.04 (m, 1H), 6.93 (m, 1H), 6.88 (m, 1H), 5.77 (s, 5H), 2.70 (m, 2H), 2.20 (s, 3H), 1.75 (s, 3H), 2.13 (m, 2H), 2.02 (m, 2H), 1.27 (t, 3H), 1.18 (t, 3H). ^{13}C NMR ($\mathrm{CDCl_3}$, δ): 243.1, 187.9, 143.3, 138.9, 128.8, 128.2, 128.1, 127.9, 127.8, 127.7, 126.93, 126.86, 126.3, 125.8, 124.4, 110.8, 27.8, 25.5, 21.5, 19.8, 15.8, 15.5. ^{11}B NMR ($\mathrm{CDCl_3}$, δ): 10.2 (d, $J = 147$ Hz, 1B), 2.6 (d, $J = 106$ Hz, 1B), -2.9 (d, $J = 142$ Hz, 1B), -17.2 (d, $J = 137$ Hz, 1B). IR ($\mathrm{CH_2Cl_2}$, cm^{-1}): 3068 (w), 2559 (s, B(H)), 2427 (w), 1589 (w), 1464 (m), 1269 (m), 1243 (m), 1061 (w), 1023 (w), 928 (w), 727 (m), 690 (s). UV−vis ($\mathrm{CH_2Cl_2}$, nm): 232. MS (CI using $\mathrm{CH_4}$): *m*/*z* 661 (base peak envelope). Anal. Calcd for $\mathrm{C_{32}H_{38}NB_4Ta}$: C, 58.16; H, 5.80; N, 2.12. Found: C, 57.61; H, 5.92; N, 2.02.

$[\mathrm{Et_2C_2B_3(C_6H_5)(CHN(2,6\text{-}Me_2C_6H_3))}]\mathrm{CpTa}(\eta^2\text{-}C,N\text{-}\mathrm{C}\{{=}\mathrm{N(2,6\text{-}Me_2C_6H_3)}\}\mathrm{C_6H_5})$ (8). Under an argon atmosphere, a solution of **7a** (100 mg, 0.151 mmol) in 5 mL of benzene was treated with 2,6-dimethylphenyl isocyanide (21 mg, 0.16 mmol), causing an immediate color change from red to red-orange. After evaporation of the solvent, the residue was dissolved in $\mathrm{CH_2Cl_2}$ and passed through a column of neutral alumina, eluting with 10:1 hexane:$\mathrm{CH_2Cl_2}$ to give 89 mg (74%) of **8** as an orange solid. X-ray quality crystals were obtained by slow evaporation from an ether/hexane solution. ^{1}H NMR ($\mathrm{C_6D_6}$, δ): 7.43 (d, $J = 6.8$ Hz, 4H), 7.18 (m, 6H), 7.11 (m, 6H), 6.98 (m, 1H), 5.74 (s, 5H), 2.70 (m, $J = 6.8$ Hz, 2H), 2.35 (s, 3H), 2.21 (s, 3H), 2.00 (s, 3H), 0.93 (s, 3H), 2.16 (m, $J = 6.8$ Hz, 4H), 2.08 (m, $J = 6.8$ Hz, 2H), 1.40 (t, $J = 6.8$ Hz, 3H), 1.16 (t, $J = 6.8$ Hz, 3H). ^{13}C NMR ($\mathrm{C_6D_6}$, δ): 230.7, 159.9, 148.9, 148.8, 143.0, 133.2, 133.1, 132.8, 132.0, 131.6, 131.5, 129.7, 129.5, 129.4, 129.2, 128.9, 128.6, 127.4, 126.4, 126.1,

Table 4. Crystallographic Data for Complexes 5a, 5b, 7a, and 8

	5a	**5b**	**7a**	**8**
empirical formula	$C_{18}H_{34}NB_4Ta$	$C_{18}H_{34}NB_4Ta$	$C_{32}H_{38}NB_4Ta$	$C_{41}H_{47}N_2B_4Ta$
fw	488.66	488.66	660.85	792.02
cryst color and habit	colorless block	colorless plate	brownish prism	red block
cryst dimens, mm	0.26 ¥ 0.34 ¥ 0.44	0.24 ¥ 0.12 ¥ 0.46	0.26 ¥ 0.20 ¥ 0.44	0.32 ¥ 0.27 ¥ 0.45
cryst syst	monoclinic	orthorhombic	monoclinic	triclinic
a, Å	8.015(3)	28.072(6)	14.565(3)	11.900(4)
b, Å	9.755(3)	30.661(7)	11.976(2)	16.918(6)
c, Å	25.644(8)	9.254(3)	16.896(5)	9.547(3)
a, deg				94.57(2)
b, deg	93.70(3)		106.24(2)	90.98(2)
g, deg				107.13(2)
V, Å^3	2001(2)	2840(2)	2830(2)	1829(2)
space group	$P2_1/n$ (No. 14)	$Fdd2$ (No. 43)	$P2_1/n$ (No. 14)	$P1$ (No. 2)
Z	4	16	4	2
D_{calc}, g cm^{-3}	1.62	1.63	1.55	1.44
radiation	Mo Ka (l = 0.710 69 Å)	Mo Ka (l = 0.710 69 Å)	Mo Ka (l = 0.710 69 Å)	Mo Ka (l = 0.710 69 Å)
m (Mo Ka), cm^{-1}	54.28	54.54	38.59	29.98
temperature, °C	−120	−120	−120	−120
2q$_{max}$	46°	50°	46°	46°
no. of reflns measd	total: 3211 unique: 2967 (R_{int} = 0.033)	total: 1934	total: 3304 unique: 3111 (R_{int} = 0.020)	total: 5380 unique: 5090 (R_{int} = 0.031)
no. of reflns with $I > 3s(I)$	1895	1624	2238	4356
no. of variables	217	216	343	450
Residuals *R*; R_w	0.027; 0.034	0.023; 0.029	0.024; 0.034	0.037; 0.052
goodness of fit	1.04	1.25	1.10	1.69
max peak in final diff map, e/Å^3	0.58	0.54	0.46	1.23 (1.11 Å from Ta)

125.6, 123.8, 49.4, 27.8, 24.2, 22.7, 19.6, 19.2, 18.7, 16.2, 16.0. ^{11}B NMR ($CDCl_3$, δ): 2.1 (s, 1B), −16.7 (d, *J* = 129 Hz, 2B), −22.3 (d, *J* = 178 Hz, 1B). IR (CH_2Cl_2, cm^{-1}): 3064 (w), 2959 (s), 2935 (s), 2867 (m), 2571, 2534, 2467 (all B(H), m), 2251 (w), 1722 (w), 1593 (s), 1470 (s), 1273 (s), 1217 (s), 922 (w), 743 (s), 768 (s), 700 (s). UV−vis (CH_2Cl_2, nm): 254 (100%), 300 (38%), 466 (4%). MS (CI using CH_4): *m/z* 792 (base peak envelope). Anal. Calcd for $C_{41}H_{47}N_2B_4Ta$: C, 62.18; H, 5.98; N, 3.54. Found: C, 62.41; H, 6.14; N, 3.71.

$[Et_2C_2B_3(C_6H_5)(CHN(2,6\text{-}Me_2C_6H_3))]CpTa[\eta^2\text{-}C,N\text{-}C\{{=}N\text{-}t\text{-}Bu\}C_6H_5]$ (9). The same procedure as for complex **8** was employed using 1 equiv of *tert*-butyl isocyanide. The purified product (70 mg, 62%) is dark yellow. ^{1}H NMR ($CDCl_3$, δ): 7.71 (d, *J* = 6.8 Hz, 2H), 7.36 (m, 2H), 7.22 (m, 2H), 7.04 (t, *J* = 5.8 Hz, 2H), 6.95 (d, *J* = 7.8 Hz, 3H), 6.81 (m, 2H), 6.75 (m, 1H), 5.81 (s, 5H), 2.51 (m, 2H), 1.94 (m, 2H), 1.90 (s, 3H), 1.76 (s, 3H), 1.16 (t, *J* = 7.8 Hz, 3H), 0.93 (t, *J* = 7.8 Hz, 3H), 0.79 (s, 9H). ^{1}H NMR (C_6D_6, δ): 7.82 (d, *J* = 7.8 Hz, 4H), 7.22 (t, *J* = 7.8 Hz, 3H), 7.06 (m, 3H), 6.97 (d, *J* = 6.8 Hz, 3H), 6.84 (d, *J* = 7.8 Hz, 3H), 6.78 (m, 1H), 5.62 (s, 5H), 2.68 (m, 2H), 2.18 (m, 1H), 2.01 (m, 1H), 2.05 (s, 6H), 1.37 (t, *J* = 6.8 Hz, 3H), 1.17 (t, *J* = 6.8 Hz, 3H), 0.63 (s, 9H). ^{13} C NMR (C_6D_6, δ): 230.5, 158.0, 151.2, 143.1, 131.5, 129.3, 129.0, 128.9, 128.7, 127.0, 126.2, 126.0, 125.6, 124.4, 123.6, 123.2, 108.3, 62.3, 28.0, 23.9, 20.8, 19.9, 16.2, 16.0, 1.6. ^{11}B NMR ($CDCl_3$, δ): −2.0 (s, 1B), −15.3 (d, *J* = 137 Hz, 2H), −20.9 (d, *J* = 163 Hz, 1B). IR (CH_2Cl_2, cm^{-1}): 3059 (m), 2967 (s), 2924 (s), 2867 (s), 2567, 2530, 2444 (all B(H), m), 2253 (w), 1736 (w), 1625 (m), 1595 (s), 1441 (s), 1367 (m), 1263 (m), 1238 (m), 1023 (m), 1097 (m), 918 (s), 820 (s), 746 (m). UV−vis (CH_2Cl_2, nm): 246 (100%), 330 (22%), 420 (3%). MS (CI using CH_4): *m/z* 743 (base peak envelope). Anal. Calcd for $C_{37}H_{47}N_2B_4Ta$: C, 59.73; H, 6.37; N, 3.76. Found: C, 59.89; H, 6.41; N, 3.88.

X-ray Crystallography. X-ray measurements were carried out on a Rigaku AFC6S diffractometer using Mo Kα radiation (λ = 0.71069 Å). Calculations were performed on a VAXstation 3500 computer using the TEXSAN 5.0 software[54] and in the later stages on a Silicon Graphics Indigo 2 Extreme computer with the teXsan 1.7 package. Relevant crystallographic data are listed in Table 4. Unit cell dimensions were determined by applying the setting angles of 25 high-angle reflections. Three standard reflections were monitored during the data collection, showing no significant variance. The intensities were corrected for absorption by applying Ψ scans of several reflections with the following transmission factors: **5a,** 0.61−1.00; **5b**, 0.40−1.00; **7a**, 0.66−1.00; **8**, 0.54−1.00. The structures **5a** and **7a** were solved by Patterson and Fourier techniques; structures **5b** and **8** were solved by direct methods in SIR88.[55] Full-matrix least-squares refinement was carried out with anisotropic thermal displacement parameters for all non-hydrogen atoms. The hydrogen atoms were found in difference Fourier maps and were included in the calculations without further refinement, except for those in structure **8** attached to atoms B4, B6, B7, and C25. These hydrogen atoms were refined with isotropic thermal parameters. The final difference maps for **5a**, **5b**, and **7** were featureless. The final electron density map for **8** showed a peak 1.23 e/A^3 high in close vicinity (1.11 Å) of the Ta atom. The results of the refinements are presented in Table 4.

Acknowledgment. Funding from the National Science Foundation (Grant No. CHE 9322490 to R.N.G. and Grant No. CHE 9313746 to M.G.F.) for partial support of this work is gratefully acknowledged.

Supporting Information Available: Tables of atomic coordinates, anisotropic displacement parameters, complete bond distances and angles, and least-squares planes for **5a**, **5b**, **7a**, and **8** (25 pages). Ordering information is given on any current masthead page.

OM9703447

---

[54] *TEXSAN 5.0: Single Crystal Structure Analysis Software*; Molecular Structure Corp.: The Woodlands, TX, 1989.

[55] Burla, M. C.; Camalli, M.; Gascarano, G.; Giacovazzo, C.; Polidori, G.; Spagna, R.; Viterbo, D. *J. Appl. Crystallogr.* **1989**, *22*, 389